Published in final edited form as:
Brain Res. 2013 June 21; 1516: 1–10. doi:10.1016/j.brainres.2013.04.020.

Ultrastructure of spines and associated terminals on brainstem neurons controlling auditory input

M. Christian Brown[a,b,*], **Daniel J. Lee**[a,b], and **Thane E. Benson**[a]

[a]Eaton-Peabody Laboratory, Massachusetts Eye and Ear Infirmary, 243 Charles Street, Boston, MA 02114, USA

[b]Department of Otology and Laryngology, Harvard Medical School, Boston, MA 02114, USA

Abstract

Spines are unique cellular appendages that isolate synaptic input to neurons and play a role in synaptic plasticity. Using the electron microscope, we studied spines and their associated synaptic terminals on three groups of brainstem neurons: tensor tympani motoneurons, stapedius motoneurons, and medial olivocochlear neurons, all of which exert reflexive control of processes in the auditory periphery. These spines are generally simple in shape; they are infrequent and found on the somata as well as the dendrites. Spines do not differ in volume among the three groups of neurons. In all cases, the spines are associated with a synaptic terminal that engulfs the spine rather than abuts its head. The positions of the synapses are variable, and some are found at a distance from the spine, suggesting that the isolation of synaptic input is of diminished importance for these spines. Each group of neurons receives three common types of synaptic terminals. The type of terminal associated with spines of the motoneurons contains pleomorphic vesicles, whereas the type associated with spines of olivocochlear neurons contains large round vesicles. Thus, spine-associated terminals in the motoneurons appear to be associated with inhibitory processes but in olivocochlear neurons they are associated with excitatory processes.

Keywords

Olivocochlear; Stapedius; Tensor tympani; Middle ear muscle; Vesicle morphometry; Electron microscopy

1. Introduction

Several groups of neurons are associated with reflexive control of processes in the auditory periphery (Liberman and Guinan, 1998). Tensor tympani (TTMN) and stapedius motoneurons (SMN), by activating their respective middle-ear muscles, control the amount of sound that is transmitted through the middle ear into the inner ear (cochlea). Medial olivocochlear (MOC) neurons, which send information from the brainstem's superior olivary complex to the cochlea, act on hair cells in the cochlea to reduce the gain of the "cochlear amplifier" and the activity of auditory nerve fibers (reviewed by Ryugo et al., 2011). Actions of all of these neurons protect the inner ear from damage caused by intense sounds and reduce the amount of masking of signals in continuous noisy backgrounds. Additionally, contraction of the middle-ear muscles during vocalization, swallowing and

*Corresponding author at: Eaton-Peabody Laboratory, Massachusetts Eye and Ear Infirmary, 243 Charles Street, Boston, MA 02114, USA. Fax: +617 720 4408. Chris_Brown@meei.harvard.edu.
Daniel_Lee@meei.harvard.edu (D.J. Lee), Thane_Benson@meei.harvard.edu (T.E. Benson).

chewing (Borg et al., 1984; Howell et al., 1986; Salomon and Starr, 1963) avoids self-stimulation that could lead to loss of sensitivity. Motoneurons and olivocochlear neurons are cholinergic, but each system has a different cranial nerve pathway for its efferent axon (tensor tympani: V3; stapedius: VII; olivocochlear: VIII).

A shared property of these auditory brainstem neurons is that they are sparsely spined (Benson and Brown, 2006; Benson et al., 2013; Lee et al., 2008; Mulders and Robertson, 2000a), but the spine documentation and comparisons of their associated synapses are incomplete. There is extensive documentation of spines on the dendrites of pyramidal cells of the cerebral cortex and neurons in the hippocampus (reviewed by Alvarez and Sabatini, 2007; Bourne and Harris, 2008). In these areas, spines range in complexity from being simple tubular structures to more complex structures that have a prominent head. At the tip, the spine usually receives a single synaptic terminal that forms an asymmetric synapse with round synaptic vesicles. Thus, the number of spines is a reflection of the glutamatergic (excitatory) input to the postsynaptic target.

In the present study, we examine the spines on auditory brainstem neurons. The results indicate that the spines have similar volume amongst the groups and have mostly simple shapes. Significantly, though, the spine-associated synapses are at various spatial positions in relation to the spine, which is a situation that is different than in cortex and hippocampus. We also provide information on the terminals associated with the spines. Using morphometry of their synaptic vesicles, we document that these brainstem neurons receive three common types of synaptic terminals. A difference between groups of neurons is in the particular type of terminal associated with the spines. For the two groups of motoneurons, the spine-associated terminals have inhibitory morphology, whereas for the MOC neurons the terminals have excitatory morphology. The results suggest that spines on these brainstem neurons are associated with particular functions that are different from those traditionally associated with spines in other systems.

2. Results

2.1. General

In ultrastructural material, labeled TTMNs, SMNs, and MOC neurons were observed to have spines that were associated with synaptic terminals. Examples of spines and terminals for each group of neurons are shown in Fig. 1. Our definition of a spine is a process emanating from a soma or a dendrite that had a length greater than, and a width less than, 0.2 μm. Spines contained flocculent material but no mitochondria. Only three spines, all from TTMNs, had a spine apparatus (Peters et al., 1991), all in their proximal portion. Our database for spines and their associated terminals is summarized in Table 1. The spines were uncommon on the soma, with a calculation of the number of spines per soma yielding from 0–40 (Table 1).

The spines deeply invaginated their associated terminals. Outlines of terminals associated with spines are shown in Fig. 2. In all cases, the spine is buried within the terminal. In most cases, a single spine was present and associated with a single terminal. However, two spines were associated with each of three separate terminals (TTMN terminal 1, MOC terminals 3 and 5), and three spines were associated with a single terminal (SMN terminal 3). Spine morphology was usually simple and lacked an obvious head (SMN terminal 1 and MOC terminal 4) although some spines swelled towards their ends (TTMN terminal 4). Their lengths were 0.75 μm or less. One spine was bi-pronged (MOC terminal 5). This spine and another that is nearby and simple are illustrated in three dimensions in a Movie of the terminal than encompasses them (Fig. 3). The Movie shows the relationship of the two spines, four synapses formed by the terminal, and a single adherens junction. Included in the

database are 4 spines of unknown origin but which were associated with terminals that synapsed on the target neurons (one TTMN and three MOC neuron spines including the one marked with an asterisk on MOC terminal 1 of Fig. 2). These spines did not differ in morphology from others in our sample.

Supplementary material related to this article can be found online at http://dx.doi.org/10.1016/j.brainres.2013.04.020.

2.2. Spine volumes

The volumes of spines for the three groups of neurons had overlapping ranges (Fig. 4). There was no significant difference between the average spine volumes (Fig. 4, Table 1) in the three groups of neurons (ANOVA p=0.152). There was also no clear difference between volume of dendritic and somatic spines (Fig. 4, see key). Most of the data are from proximal dendrites, but a single spine on an MOC distal dendrite (diam. about 0.9 μm, stained for acetylcholinesterase) had a volume of 0.021 μm^3, on the small size but within the range of volumes of the other somatic and proximal dendritic spines.

2.3. Spine synapses

Synapses were observed at variable positions on and near the spines (Fig. 2, Table 1). To qualify as a synapse, three criteria were required: a cleft between pre- and postsynaptic membrane, postsynaptic dense material, and presynaptic vesicles. About half of the spines had synapses at the spine's base (Fig. 1, MOC neuron; Fig. 2, TTMN 4). This is the case for the reconstruction shown in the Movie (Fig. 3), where each of the two spines has synapses that extend just into their bases. Two other synapses of that terminal were more remote from the spines but within 1 μm of the spine's base. This type of "remote" synapse (e.g., Fig. 2, TTMN terminal 3, SMN terminal 4, and MOC terminal 1) was the only type found in about a third of the spines (Table 1). A few synapses were along the spine's shaft (Fig. 1, TTMN and SMN; Fig. 2, TTMN terminal 1), and only one of these was near the spine's tip (Fig. 2, TTMN terminal 5). There were no obvious differences in positions of spines between TTMNs, SMNs, or MOC neurons (Table 1). None of the spines had synapses directly at their tips. Nor did any of the synapses studied here have a perforated density as has been observed in other synapses associated with spines (Calverly and Jones, 1990). Finally, adherens junctions are present in a minority of the terminals and when present their position is usually near the base of the spine (Fig. 1, SMN; Fig. 2, terminals SMN 3 and MOC 3; Fig. 3).

2.4. Morphometry of synaptic vesicles

Morphometry of vesicles was previously used to separate synaptic terminals on TTMNs (Benson et al., 2013), and here that type of analysis is extended to terminals on SMNs and MOC neurons. The approach is shown for one TTMN terminal in Fig. 5. Individual vesicles from a single terminal had a wide range of areas and circularities, and this range was compressed by calculating mean data for all the vesicles and synapses of a particular terminal (Fig. 5, plot). The mean data, where each point represents a single synaptic terminal, are plotted in Fig. 6. The data fit our visual impression and previous reports (Benson and Brown, 2006; Benson et al., 2013; Lee et al., 2008) that there are three types of terminals with non-overlapping mean values. Using the k-means analysis (Fig. 6 legend, Experimental Procedures) with an assumption of three types yields a separation plotted as the three colors on Fig. 6. On all three groups of neurons, pleomorphic (Pleo) vesicles had mean circularities less than 0.85, whereas the other types have higher mean circularity (more round in shape). Small round (Sm Rnd) vesicles have mean areas generally less than 1,400 nm^2, whereas large round (Lg Rnd) vesicles have mean areas that are greater. Although it is not plotted, another characteristic that separates the two round-vesicle terminals from the

Pleo-vesicle terminals is that the former have synapses with distinct postsynaptic densities (asymmetric synapses) whereas the latter have synapses with less distinct densities so they are more symmetric (Fig. 1). Two rare types of terminals on motoneurons, those with vesicles of heterogenous sizes or with a postsynaptic cistern, were not part of this analysis (Benson et al., 2013; Lee et al., 2008).

For each group of neurons, it is clear that spine-associated terminals (Fig. 6, filled symbols) are of a particular type. For motoneurons, spine-associated terminals have Pleo vesicles, whereas for MOC neurons, these terminals have Lg Rnd vesicles. In fact, all terminals with Lg Rnd vesicles on MOC neurons were associated with spines except one (Fig. 6A, orange open circle), and this terminal was comparatively small (approximately a sphere about 0.8 μm in diameter). Almost all of this terminal was examined in its apposition to the MOC neuron (in 11 serial sections), so we are confident that it was not associated with a spine. For the most part, the MOC terminals were sectioned through their entirety (21 of the 34 terminals plotted on Fig. 6C). On the motoneurons, though, due to shorter series of sections, many of the terminals were not completely sectioned and there could have been spines in the unsampled portions. Our best data here are from TTMNs, where five of the Pleo terminals were examined in 12–20 sections and spines were not observed. The overall data indicate that about 1/3 of the motoneuron Pleo terminals are associated with spines. Comparison of those Pleo terminals associated with spines vs. those not associated did not reveal any differences in size of terminal, mitochondrial content, or other features.

3. Discussion

3.1. Morphology of spines on brainstem neurons

In this report, we document the spines from three groups of auditory neurons that reside in the brainstem, and we show that each is associated with a particular type of synaptic terminal. Outside our laboratory, only one previous report (Mulders and Robertson, 2000a) described spines on an MOC neuron that was labeled with Fluorogold and examined in the light microscope. Those spines were not associated with peptidergic or adrenergic terminals. The number of spines per neuron was not given in that study, but they suggest that spines became more numerous on the distal dendrites, which were generally not available in our study. Earlier-used tracers such as HRP probably did not fill spines of TTMNs (Billig et al., 2007; Itoh et al., 1986; Keller et al., 1983; Lyon, 1975; Mizuno et al., 1982; Rouiller et al., 1986; Shaw and Baker, 1983; Spangler et al., 1982; Strutz et al., 1988; Thompson et al., 1998) or SMNs (Lyon, 1978; Rouiller et al., 1989; Shaw and Baker, 1983; Thompson et al., 1998).

The spines on our three groups of brainstem neurons were not significantly different in volume, nor do they differ in volume from spines on cortical neurons. The volumes of brainstem neuron spines (avg. 0.065–0.140 μm^3) are on the order of those previously reported for visual cortex pyramidal cells by Freire (1978) and by Arellano et al. (2007), which average 0.12 μm^3 and 0.09 μm^3, respectively, and for CA1 pyramidal cells by Harris and Stevens (1989), which average 0.06 μm^3. Spine apparatus have been found previously in many spines with heads but only in a minority of spines lacking a head (Arellano et al., 2007). In the present study, most of the spines lacked a head and only a few had a spine apparatus. Spines are also present on other auditory brainstem neurons. For example, in the cochlear nucleus, multipolar, octopus, and fusiform cells all have some form of spines (Brawer et al., 1974; Kane, 1973; Kane, 1974; Smith and Rhode, 1985), as do several types of neurons in the inferior colliculus (Oliver et al., 1991).

3.2. Specific types of terminals are associated with spines

Morphometric data presented here suggest that TTMNs, SMNs, and MOC neurons each receive three separate types of terminals. Previous studies of SMNs and MOC neurons have separated the synaptic vesicles by visual inspection (Benson and Brown, 2006; Helfert et al., 1988; Lee et al., 2008; Spangler et al., 1986; White, 1984). The new data show in a quantitative way that TTMN and SMN spines are only associated with terminals containing Pleo synaptic vesicles, which are the terminals that form symmetric synapses. This type of synapse is likely to use one or both of the inhibitory neurotransmitters glycine or GABA (Örnung et al., 1998;Rubio, 2004; Torrealba and Carrasco, 2004; Uchizono, 1965). The number of spines does not reflect the number of inhibitory inputs because some Pleo vesicle terminals lack associated spines. Perhaps spineless Pleo terminals result from fluidity in the formation / retraction of spines (Alvarez and Sabatini, 2007). Elsewhere in the brain, inhibitory terminals associated with spines are rare but are found in the visual cortex (Colonnier, 1968), and, along with excitatory inputs, can be found on some spines in the cortical barrel fields (Knott et al., 2002) and in the dentate fascia (Fifková et al., 1992). In the case of the middle ear muscle reflex, the reflex is driven by excitatory input, which means that the spine-associated inhibitory synapses perform a modulatory role rather than drive the reflex.

In contrast, MOC neuron spines are associated with terminals containing Lg Rnd vesicles that form asymmetric synapses. This type of synapse is likely to use the excitatory neurotransmitter glutamate (Örnung et al., 1998; Rubio, 2004; Torrealba and Carrasco, 2004; Uchizono, 1965). Although in some neurons with excitatory spine inputs, the number of spines reflects the number of excitatory inputs, that simple conclusion cannot be made for MOC neurons. That is because these neurons receive another terminal type (with Sm Rnd vesicles) that is also presumably excitatory but that is not associated with spines. Those terminals are likely to originate in the cochlear nucleus, in multipolar cells that project to MOC neurons and drive their excitatory response to sound (Thompson and Thompson, 1991a,1999b; de Venecia et al., 2005; Darrow et al. 2012). Thus, the terminals with Lg Rnd vesicles are likely to modulate the reflexive response to sound, and they may originate in descending inputs to MOC neurons from the inferior colliculus (Vetter et al., 1993) or auditory cortex (Mulders and Robertson, 2000b).

One caveat with our findings is that in the case of the Pleo terminals on TTMNs and SMNs, our ability to detect symmetric synapses onto spines is limited. The cleft of these synapses may be less obvious because the small and round nature of the spines allows less comparison between synaptic and adjacent non-synaptic membranes compared to an uncurved portion the membrane. If in fact we missed synapses in these cases there may be a closer association of synapses with spines than we report here. We have more confidence in our ability to detect spine-associated synapses on MOC neurons because they are asymmetric and thus more visible. Even here, though, they were also not usually found along the spine (Figs. 2 and 3). Thus, for the brainstem neurons examined here, spines appear less poised to carry out the compartmentalization of the various processes associated with the action of the spine synapse elsewhere (reviewed by Chen and Sabatini, 2012).

3.3. Function of Spines on brainstem Neurons

Spines have been associated with synaptic plasticity (Bourne and Harris, 2008; Calverly and Jones, 1990; Yuste and Bonhoeffer, 2001). For example, whisker stimulation increases the number of spines and the density of spine-associated synapses in the cortical barrel corresponding to the stimulated whisker but not to other barrels (Knott et al., 2002). Activity of MOC neurons, as measured in humans with tests using otoacoustic emissions, increases during daily training on a speech-in-noise discrimination task (de Boer and Thornton, 2008).

Plastic changes in MOC responses have been shown after the animal is exposed to moderate-level sound for two weeks in a paradigm called “sound conditioning” (Brown et al., 1998). Compared to controls, the MOC neurons in conditioned guinea pigs have higher firing rates in response to binaural noise. It is not clear what part of the MOC input pathway is changed, but one idea is that MOC plasticity involves the terminals associated with spines, which could up-regulate their excitation. These spine-associated terminals may originate in higher centers (Benson and Brown, 2006). On motoneurons of the middle ear muscles, the spines are associated with Pleo terminals, so if there is plasticity in motoneurons, it is likely to be reflected by changes in inhibition. The distinct association of spines and synapses reported here suggests one focus for future investigations of changes associated with plasticity in these systems.

4. Experimental procedures

4.1. Animals

All experimental procedures on animals were performed in accordance with the National Institutes of Health guidelines for the care and use of laboratory animals as well as approved animal care and use protocols at the Massachusetts Eye and Ear Infirmary. The material for this study was compiled from our previous studies of brainstem neurons (Benson and Brown, 2006; Benson et al., 2013; Lee et al., 2008). TTMN and SMN material was from adult Sprague–Dawley rats (a species that has a robust middle ear muscle reflex to sound (Relkin et al., 2005) and have been the subject of previous retrograde labeling studies (Billig et al., 2007; Reuss et al., 2008; Reuss et al., 2009; Rouiller et al., 1986; Rouiller et al., 1989; Spangler et al., 1982). MOC material was from adult guinea pigs (which have a robust MOC reflex to sound (Kujawa and Liberman, 2001) vs. a weak middle ear muscle reflex to sound (Avan et al., 1992) and have been studied by retrograde labeling (Robertson, 1985; Strutz, 1981). The number of rats used for electron microscopy was 2 for TTMNs and 3 for SMNs, and the number of guinea pigs was 4.

4.2. Labeling

The methods were described previously (Benson and Brown, 2006; Benson et al., 2013; Lee et al., 2008). Injections of 30% horseradish peroxidase were made into the tensor tympani muscle or stapedius muscle or cochlea (3 of the guinea pigs). After a survival time of 24 h, the animals were re-anesthetized and perfused with 0.1% sodium nitrite in physiologic saline followed by 0.5% paraformaldehyde and 1% glutaraldehyde in 0.1 M cacodylate buffer, which was then followed by 0.5% paraformaldehyde and 3% glutaraldehyde in buffer. The total fixation time was 2 h. The brainstem was blocked, embedded in a gelatin–albumin mixture hardened with 2.3% glutaraldehyde, and sectioned (80 μm thickness, transverse plane) using a Vibratome. The sections were soaked in a solution of tetramethylbenzidine and ammonium heptamolybdate (Olucha et al., 1985) in 0.1 M phosphate buffer made hypertonic with dextrose. Hydrogen peroxide (0.3%, 1 ml/100 ml) was then added every five minutes for twenty minutes. The sections were moved to fresh incubation solution and H_2O_2 again added to allow a more dense reaction product with minimal crystal artifact. Selected sections with labeled TTMNs were treated overnight with hypertonic OsO_4 (pH 5 at 3 °C, (Henry et al., 1985). The sections were stained en bloc with filtered 1% uranyl acetate (overnight at 3 °C), dehydrated with methanol through propylene oxide, infiltrated with epoxy and flat-embedded between two transparent sheets of Aclar (Pro Plastics, Wall, NJ). One uninjected guinea pig brainstem was stained for acetylcholinesterase instead of retrograde labeling to examine MOC dendrites farther away from the cell body than the reaction product typically extends. The acetylcholinesterase stain was modified from the original version (Brown and Levine, 2008) as described by (Brown and Levine, 2008; Osen et al., 1984), We studied this labeled dendrite from the ventral nucleus of the trapezoid body,

where the distribution of stained neurons is near-identical to the distribution of retrogradely labeled MOC neurons (Osen, 1969; Osen et al., 1984; Warr, 1975).

Labeled TTMNs were examined from the trigeminal motor nucleus and labeled SMNs were examined from the ventro-medial perifacial area, both ipsilateral to the injected muscle. Labeled MOC neurons were examined from the ventral nucleus of the trapezoid body contralateral to the injection (where the majority of MOC neurons are located).

4.3. Electron microscopy

After examination in the light microscope, the material was ultrathin sectioned. Section thickness was presumed to be 80 nm because of the silver-gold color of the sections (Sakai, 1980). The sections were examined with the transmission electron microscope and a correlation between the light- and electron-microscopic images was made. In order to determine whether terminals formed several synapses, each terminal was assigned an identifier and followed through the serial sections. A terminal was considered partially sectioned if it continued beyond the sections available and completely sectioned if its apposition with the TTMN tapered off to a small process within the available sections. The distinction between synaptic terminal position (soma vs. proximal dendrite) was made on the basis of tapering of the soma into the dendrite and whether organelles are oriented circumferentially around the nucleus in the soma vs. parallel to the axes of dendrites. Representations of spinous terminals (e.g., Fig. 2) were generated as follows: For terminals with a single spine, the largest terminal cross-section including part of the spine was traced. Serial sections were aligned and the entire spine (or as much as was available) reconstructed. For terminals with multiple spines, the cross-section tracing was modified in the vicinity where spines invaginated the terminal. Calculations of the total number of spines/soma were based on the number of spines observed in our series (0–4 for three TTMNs, 3 each for two SMNs, and 4–5 for two MOC neurons), the percentage of the soma examined (10–24% for TTMNs, 10–12% for SMNs, and 24–26% for MOC neurons), measurement of the soma diameter, and the assumption of an oblate spheroid for the soma shape.

4.4. Vesicle morphometry

Morphometric data on synaptic vesicles were obtained from images of 21,000–25,000x original magnification. Vesicles were traced along the outer edges of their membranes using a digitizing tablet (e.g., Fig. 5B). ImageJ was used to compute vesicle area and circularity (4π(area/perimeter^2)) (Montero and Bribiesca, 2009). As defined this way, circularity ranges from 0 to 1 (for a circle, circularity is 1.0 and for an ellipse with a major axis twice that of its minor axis, it is 0.84). Vesicles were measured in up to 6 sections per synapse, and data for all available synapses were combined for each terminal for Fig. 6. Due to the fact that vesicular data fell over a wide range, it was necessary to analyze a large number of vesicles for each terminal (18–103 vesicles, all of which were within 250–800 nm from the presynaptic membrane adjacent to the density). We excluded from the data set 10 terminals with fewer than 18 vesicles; these terminals were usually small, partially documented terminals at the beginning or end of the series of sections, or in one instance a terminal whose volume was taken up by a mitochondrion leaving little space for vesicles. The k-means clustering algorithm (implemented as the *kmeans* function in MATLAB) was used to provide an objective method for dividing the morphometric data (Benson et al., 2013). Data were normalized on a scale from 0 to 1 before the analysis was performed.

A reconstruction of one terminal and associated spines (Fig. 3) was made by outlining the serial sections and associated structures (synapses, adherens junctions), which were digitized and entered into Amira 3.1 (Mercury Compute Systems, San Diego, CA) as a size-calibrated

image stack. Alignment of the outlines was with the autoalign feature of Amira. A polygonal surface model was generated, simplified, and smoothed by other Amira subroutines.

Supplementary Material

Refer to Web version on PubMed Central for supplementary material.

Acknowledgments

We thank Dr. Bernardo Sabatini for comments on an earlier draft of the manuscript, Dr. Wen Xu and Marie Drottar for technical assistance, Haobing Wang for help with the Amira reconstruction, and Amelie Guex for the MATLAB kmeans implementation.

Grant sponsor: National Institutes of Health-NIDCD, grant numbers DC01089 (to M.C.B.) and DC06285 (to D.J.L.).

REFERENCES

Alvarez VA, Sabatini BL. Anatomical and physiological plasticity of dendritic spines. Ann. Rev. Neurosci. 2007; 30:79–97. [PubMed: 17280523]

Arellano JI, Benavides-Piccione R, DeFelipe J, Yuste R. Ultrastructure of dendritic spines: correlation between synaptic and spine morphologies. Front. Neurosci. 2007; 1:131–143. [PubMed: 18982124]

Avan P, Loth D, Menguy C, Teyssou M. Hypothetical roles of middle ear muscles in guinea-pig. Hear. Res. 1992; 59:59–69. [PubMed: 1629047]

Benson TE, Brown MC. Ultrastructure of synaptic input to medial olivocochlear neurons. J. Comp. Neurol. 2006; 499:244–257. [PubMed: 16977616]

Benson TE, Lee DJ, Brown MC. Tensor tympani motoneurons receive mostly excitatory synaptic inputs. Anat. Rec. 2013; 296:133–145.

Billig I, Yeager MS, Blikas A, Raz Y. Neurons in the cochlear nuclei controlling the tensor tympani in the rat: a study using pseudorabies virus. Brain Res. 2007; 1154:124–136. [PubMed: 17482147]

Borg, E.; Counter, SA.; Rosier, G. Theories of middle ear muscle functions. In: Silman, S., editor. The Acoustic Reflex: Basic Principles and Clinical Applications. Academic Press; Orlando: 1984. p. 63-101.

Bourne JN, Harris KM. Balancing structure and function at hippocampal dendritic spines. Ann. Rev. Neurosci. 2008; 31:47–67. [PubMed: 18284372]

Brawer JR, Morest DK, Kane EC. The neuronal architecture of the cochlear nucleus of the cat. J. Comp. Neurol. 1974; 155:251–300. [PubMed: 4134212]

Brown MC, Kujawa SG, Liberman MC. Single olivocochlear neurons in the guinea pig: II. Response plasticity due to noise conditioning. J. Neurophysiol. 1998; 79:3088–3097. [PubMed: 9636110]

Brown MC, Levine JL. Dendrites of medial olivocochlear (MOC) neurons in mouse. Neuroscience. 2008; 154:147–159. [PubMed: 18313859]

Calverly RKS, Jones DG. Contributions of dendritic spines and perforated synapses to synaptic plasticity. Brain Res. Rev. 1990; 15:215–249. [PubMed: 2289086]

Chen Y, Sabatini BL. Signaling in dendritic spines and spine microdomains. Curr. Opinion Neurobiol. 2012; 22:389–396.

Colonnier M. Synaptic patterns on different cell types in the different laminae of the cat visual cortex. an electron microscope study. Brain Res. 1968; 9:268–287. [PubMed: 4175993]

Darrow KN, Benson TE, Brown MC. Planar multipolar cells in the cochlear nucleus project to medial olivocochlear neurons in mouse. J. Comp. Neurol. 2012; 520:1365–1375. [PubMed: 22101968]

de Boer E, Thornton AR. Neural correlates of perceptual learning in the auditory brainstem: efferent activity predicts and reflects improvement at a speech-in-noise discrimination task. J. Neurosci. 2008; 28:4929–4937. [PubMed: 18463246]

de Venecia RK, Liberman MC, Guinan JJ Jr. Brown MC. Medial olivocochlear reflex interneurons are located in the posteroventral cochlear nucleus. J. Comp. Neurol. 2005; 487:345–360. [PubMed: 15906311]

Fifková E, Eason H, Schaner P. Inhibitory contacts on dendritic spines of the dentate fascia. Brain Res. 1992; 577:331–336. [PubMed: 1606504]

Freire M. Effects of dark rearing on dendritic spines in layer IV of the mouse visual cortex. A quantitative electron microscopical study. J. Anat. 1978; 126:193–201. [PubMed: 649498]

Harris KM, Stevens KJ. Dendritic spines of CA1 pyramidal cells in the rat hippocampus: serial electron microscopy with reference to their biophysical characteristics. J. Neurosci. 1989; 9:2982–2997. [PubMed: 2769375]

Helfert RH, Schwartz IR, Ryan AF. Ultrastructural characterization of gerbil olivocochlear neurons based on differential uptake of 3H-d-Aspartic acid and a wheatgerm agglutinin-horseradish peroxidase conjugate from the cochlea. J. Neurosci. 1988; 8:3111–3123. [PubMed: 3171669]

Henry MA, Westrum LE, Johnson LR. Enhanced ultrastructural visualization of the horseradish peroxidase-tetramethylbenzidine reaction product. J. Histochem. Cytochem. 1985; 33:1256–1259. [PubMed: 4067278]

Howell P, Marchbanks RJ, El-Yaniv N. Middle ear muscle activity during vocalization in normal speakers and stutterers. Acta Otolaryngol. 1986; 102:396–402. [PubMed: 3788538]

Itoh K, Nomura S, Konishi A, Yasui Y, Sugimoto T, Muzino N. A morphological evidence of direct connections from the cochlear nuclei to tensor tympani motoneurons in the cat: a possible afferent limb of the acoustic middle ear reflex pathways. Brain Res. 1986; 375:214–219. [PubMed: 2424568]

Kane EC. Octopus cells in the cochlear nucleus of the cat: heterotypic synapses upon homeotypic neurons. Intern. J. Neurosci. 1973; 5:251–279.

Kane EC. Synaptic organization in the dorsal nucleus of the cat: a light and electron microscopic study. J. Comp. Neurol. 1974; 155:301–329. [PubMed: 4836032]

Keller JT, Saunders MC, Ongkiko CM, Johnson J, Frank E, Van Loveren H, Tew JMJ. Identification of motoneurons innervating the tensor tympani and tensor veli palatini muscles in the cat. Brain Res. 1983; 270:209–215. [PubMed: 6883092]

Knott GW, Quairiaux CG, Welker E. Formation of dendritic spines with GABAergic synapses induced by whisker stimulation in adult mice. Neuron. 2002; 34:265–273. [PubMed: 11970868]

Kujawa S, Liberman MC. Effects of olivocochlear feedback on distortion product otoacoustic emissions in guinea pig. J. Assoc. Res. Otolaryngol. 2001; 2:268–278. [PubMed: 11669399]

Lee DJ, Benson TE, Brown MC. Diverse synaptic terminals on rat stapedius motoneurons. J. Assoc. Res. Otolaryngol. 2008; 9:321–333. [PubMed: 18563488]

Liberman MC, Guinan JJ Jr. Feedback control of the auditory periphery: anti-masking effects of middle ear muscles vs. olivocochlear efferents. J. Commun. Disord. 1998; 31:471–483. [PubMed: 9836136]

Lyon M. The central location of the motor neurons to the stapedius muscle in the cat. Brain Res. 1978; 143:437–444. [PubMed: 348268]

Lyon MJ. Localization of the efferent neurons of the tensor tympani muscle of the newborn kitten using horseradish peroxidase. Exp. Neurol. 1975; 49:439–455. [PubMed: 1193198]

Mizuno N, Nomura S, Konishi A, Sumi MU, Takahashi O, Yasui Y, Takada M, Matsushima R. Localization of motoneurons innervating the tensor tympani muscles: an horseradish peroxidase study in the guinea pig and cat. Neurosci. Lett. 1982; 31:205–208. [PubMed: 7133555]

Montero RS, Bribiesca E. State of the art of compactness and circularity measures. Internat. Math. Forum. 2009; 4:1305–1335.

Mulders WHAM, Robertson D. Morphological relationships of peptidergic and noradrenergic nerve terminals to olivocochlear neurones in the rat. Hear. Res. 2000a; 144:53–64. [PubMed: 10831865]

Mulders WHAM, Robertson D. Evidence for direct cortical innervation of medial olivocochlear neurones in rats. Hear. Res. 2000b; 144:65–72. [PubMed: 10831866]

Oliver DL, Kuwada S, Yin TCT, Haberly LB, Henkel CK. Dendritic and axonal morphology of HRP-injected neurons in the inferior colliculus of the cat. J. Comp. Neurol. 1991; 303:75–100. [PubMed: 2005240]

Olucha F, Martinez-Garcia F, Lopez-Garcia C. A new stabilizing agent for the tetramethyl benzidine (TMB) reaction product in the histochemical detection of horseradish peroxidase (HRP). J. Neurosci. Methods. 1985; 13:131–138. [PubMed: 3999803]

Örnung G, Ottersen O, Cullheim S, Ulfhake B. Distribution of glutamate-, glycine-, and GABA-immunoreactive nerve terminals on dendrites in the cat spinal motor nucleus. Exp. Brain Res. 1998; 118:517–532. [PubMed: 9504847]

Osen KK. Cytoarchitecture of the cochlear nuclei in the cat. J. Comp. Neurol. 1969; 136:453–484. [PubMed: 5801446]

Osen KK, Mugnaini E, Dahl A-L, Christiansen AH. Histochemical localization of acetylcholinesterase in the cochlear and superior olivary nuclei. a reappraisal with emphasis on the cochlear granule cell system. Arch. Ital. Biol. 1984; 122:169–212. [PubMed: 6517650]

Peters, A.; Palay, SL.; Webster, HF. The Fine Structure of the Nervous System. Oxford; New York: 1991.

Relkin EM, Sterns W, Azeredo WJ, Prieve BA, Woods CI. Physiological mechanisms of onset adaptation and contralateral suppression of DPOAEs in the rat. J. Assoc. Res. Otolaryngol. 2005; 6:119–135. [PubMed: 15952049]

Reuss S, Al-Butmeh S, Riemann R. Motoneurons of the stapedius muscle in the guinea pig middle ear: afferent and efferent transmitters. Brain Res. 2008; 1221:59–65. [PubMed: 18554578]

Reuss S, Kuhn I, Windoffer R, Riemann R. Neurochemistry of identified motoneurons of the tensor tympani muscle in rat middle ear. Hear. Res. 2009; 248:69–79. [PubMed: 19126425]

Robertson D. Brainstem location of efferent neurons projecting to the guinea pig cochlea. Hear. Res. 1985; 20:79–84. [PubMed: 2416731]

Rouiller EM, Capt M, Dolivo M, de Ribaupierre F. Tensor tympani reflex pathways studied with retrograde horseradish peroxidase and transneuronal viral tracing techniques. Neurosci. Lett. 1986; 72:247–252. [PubMed: 3029633]

Rouiller EM, Capt M, Dolivo M, de Ribaupierre F. Neuronaδl organization of the stapedius reflex pathways in the rat: a retrograde HRP and viral transneuronal tracing study. Brain Res. 1989; 476:21–28. [PubMed: 2464420]

Rubio ME. Differential distribution of synaptic endings containing glutamate, glycine, and GABA in the rat dorsal cochlear nucleus. J. Comp. Neurol. 2004; 477:253–272. [PubMed: 15305363]

Ryugo, DK.; Fay, RR.; Popper, AN. Aud. Vestibular Efferents. Vol. vol 38. Springer Science +Business Media, LLC; New York: 2011.

Salomon G, Starr A. Electromyography of middle ear muscles in man during motor activities. Acta Neurol. Scand. 1963; 39:161–168. [PubMed: 13991171]

Shaw MD, Baker R. The locations of stapedius and tensor tympani motoneurons in the cat. J. Comp. Neurol. 1983; 216:10–19. [PubMed: 6306062]

Smith PH, Rhode WS. Electron microscopic features of physiologically characterized, HRP-labeled fusiform cells in the cat dorsal cochlear nucleus. J. Comp. Neurol. 1985; 237:127–143. [PubMed: 4044890]

Spangler KM, Henkel CK, Miller IJ Jr. Localization of the motor neurons to the tensor tympani muscle. Neurosci. Lett. 1982; 32:23–27. [PubMed: 6183622]

Spangler KM, White JS, Warr WB. Electron microscopic features of axon terminals on olivocochlear neurons in the cat. Assoc. Res. Otolaryngol. (Abstr.). 1986; 9:37–38.

Strutz J. Efferent innervation of the cochlea. Ann. Otol. 1981; 90:158–160.

Strutz J, Münker G, Zöllner C. The motor innervation of the tympanic muscles in the guinea pig. Arch. Otorhinolaryngol. 1988; 245:108–111. [PubMed: 3390073]

Thompson AM, Thompson GC. Posteroventral cochlear nucleus projections to olivocochlear neurons. J. Comp. Neurol. 1991a; 303:267–285. [PubMed: 2013640]

Thompson AM, Thompson GC. Projections from the posteroventral cochlear nucleus to the superior olivary complex in the guinea pig: light and EM observations with the PHA-L method. J. Comp. Neurol. 1991b; 311:495–508. [PubMed: 1757599]

Thompson AM, Thompson GC, Britton BH. Serotoninergic innervation of stapedial and tensor tympani motoneurons. Brain Res. 1998; 787:175–178. [PubMed: 9518599]

Torrealba F, Carrasco M. A review on electron microscopy and neurotransmitter systems. Brain Res. Rev. 2004; 47:5–17. [PubMed: 15572159]

Uchizono K. Characteristics of excitatory and inhibitory synapses in the central nervous system of the cat. Nature. 1965; 207:642–643. [PubMed: 5883646]

Vetter DE, Saldana E, Mugnaini E. Input from the inferior colliculus to medial olivocochlear neurons in the rat: A double label study with PHA-L and cholera toxin. Hear. Res. 1993; 70:173–186. [PubMed: 8294262]

Warr WB. Olivocochlear and vestibular efferent neurons of the feline brainstem: Their location, morphology, and number determined by retrograde axonal transport and acetylcholinesterase histochemistry. J. Comp. Neurol. 1975; 161:159–182. [PubMed: 47866]

White JS. Fine structure of medial olivocochlear neurons in the rat. Soc. Neurosci. (Abstr.). 1984; 10:393.

Yuste R, Bonhoeffer T. Morphological changes in dendritic spines associated with long-term synaptic plasticity. Ann. Rev. Neurosci. 2001; 24:1071–1089. [PubMed: 11520928]

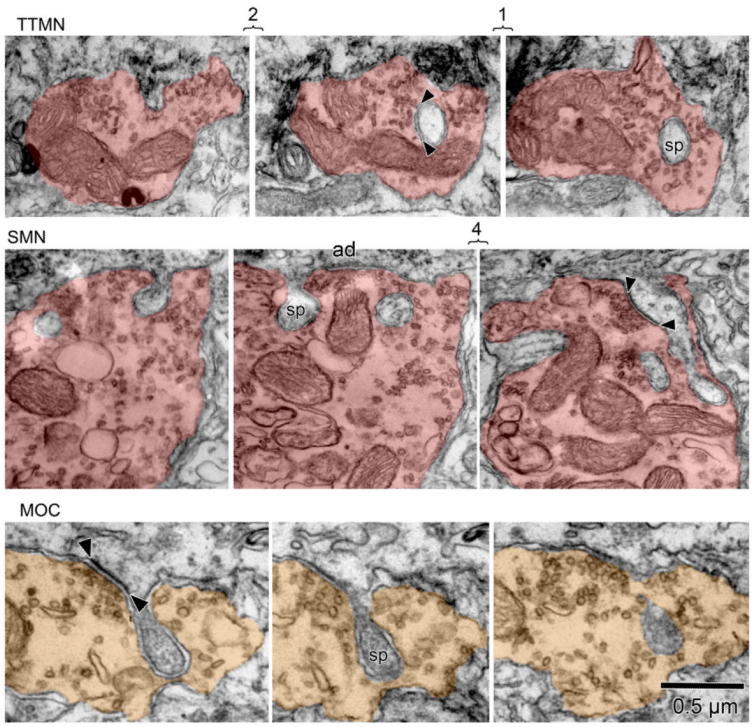

Fig. 1.

Electron micrographs from a labeled tensor tympani motoneuron (TTMN), a labeled stapedius motoneuron (SMN), and a labeled medial olivocochlear (MOC) neuron, all uncolored and towards the top of the panels, with their associated spines (sp) and spine-associated terminals (colored structures). In each case, a spine (sp) invaginates the terminal. The illustrated sections are consecutive serial sections unless brackets are present, in which case the numbers indicate how many sections are skipped. Arrowheads illustrate synapses; ad denotes adherens junction. Our criteria for a synapse are illustrated: (1) a cleft between pre- and postsynaptic membrane, postsynaptic dense material, and synaptic vesicles. The spine-associated synapses received by TTMNs and SMNs have minimal postsynaptic dense material, making them symmetric in appearance.

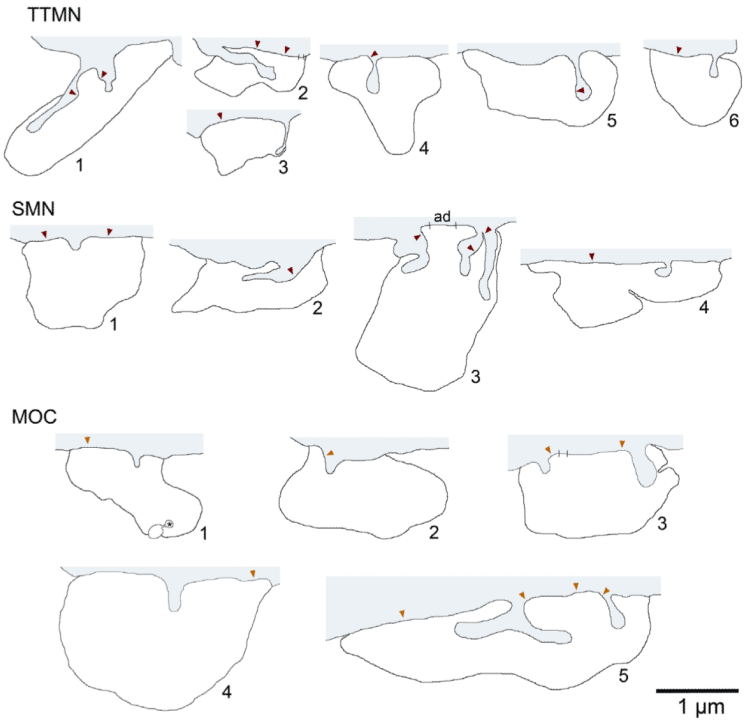

Fig. 2.

Schematic representations of spine-associated terminals from the three groups of neurons. In each case, gray shading at the top indicates the target neuron and its spine(s), and the white outline below indicates the spine-associated terminal. Red arrowheads mark centers of synapses. Hatch marks delineate adherens junctions (the one on SMN terminal 3 marked "ad"). The adherens junction on MOC terminal 5 was not indicated for clarity - it is "behind" the bi-pronged spine (see Fig. 3). One terminal (MOC terminal 1) had an additional spine (asterisk) that originated from an unknown source. Three of the terminals illustrated here also appear in Fig. 1 (TTMN terminal 5, SMN terminal 3, and MOC terminal 5). MOC terminal 4 was the only terminal from an AChE-stained case, and appeared on a distal dendrite.

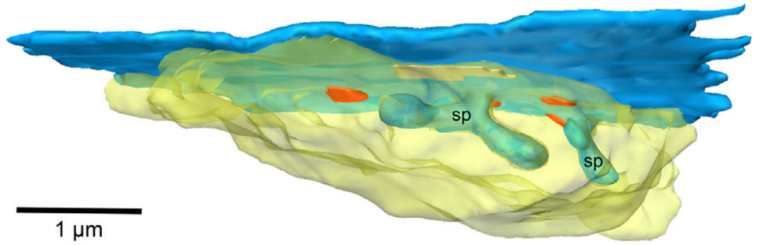

Fig. 3.

Still from a Movie of a reconstruction of two spines and adjacent part of an MOC neuron (blue color). The associated synaptic terminal (translucent yellow) forms four synapses (red color), two of which are at the bases of the spines and two of which are more remote. An adherens junction is also formed (opaque yellow color). A two-dimensional image of this terminal is pictured in Fig. 2 (MOC terminal 5). The reconstruction is composed of 26 serial sections. Still image is modified from (Benson and Brown, 2006). A video clip is available online. Supplementary material related to this article can be found online at http://dx.doi.org/10.1016/j.brainres.2013.04.020

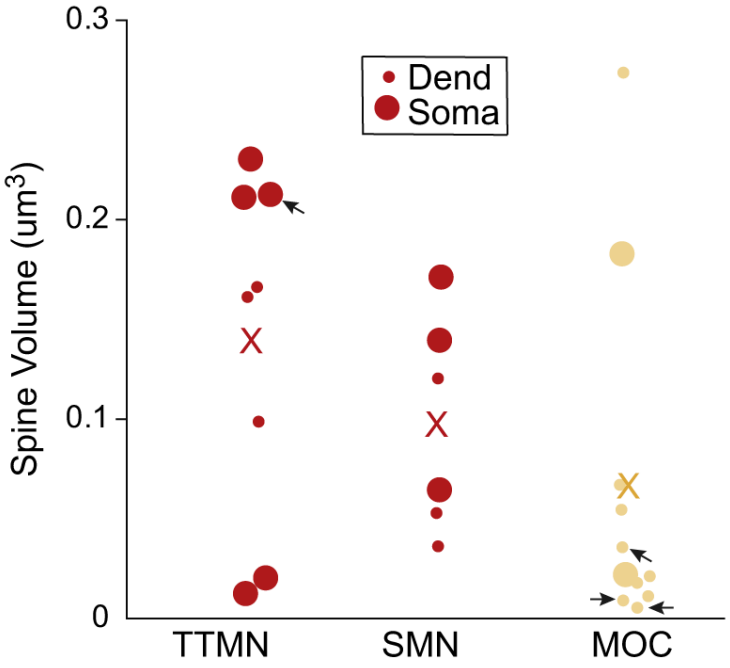

Fig. 4.

Spine volumes for spines from TTMNs, SMNs, and MOC neurons. Large symbols represent spines from somata and small symbols represent those for dendrites (see key). X's indicate average spine volume for each neuron group. Four arrows point to symbols denoting spines of unknown origin that were included because they invaginated terminals synapsing on a TTMN or an MOC neuron.

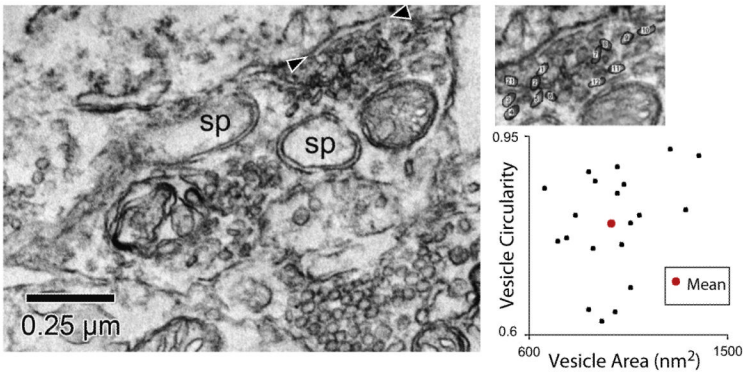

Fig. 5.

Electron micrograph of a TTMN (upper left part of image) receiving a synapse (arrowheads) from a terminal (lower part of image) that contains pleomorphic synaptic vesicles. This terminal envelopes a spine (sp) seen here in two portions. Inset shows a portion of the terminal with some of the synaptic vesicles circled and numbered for analysis. Plot shows the circularity vs. area for individual vesicles of this terminal. The large dot indicates the mean area and mean circularity for the vesicles of this terminal. Such mean data are plotted in Fig. 6. This terminal is pictured in Fig. 2 (TTMN terminal 2).

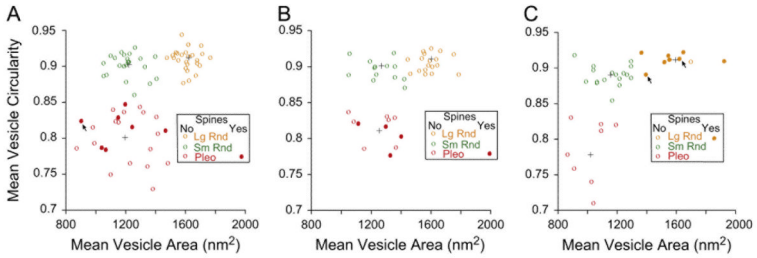

Fig. 6.

Morphometric data for synaptic vesicles in terminals on TTMNs (A), SMNs (B), and MOC neurons (C). Each point represents mean data for all measured vesicles (see Fig. 5) and all synapses from a single terminal. In each panel, three clusters, large and round (Lg Rnd, orange), small and round (Sm Rnd, green), and pleomorphic (Pleo, red), are identified by the kmeans algorithm (see Experimental Procedures) and the centroid of each cluster is shown by a black cross. Spine-associated terminals (filled symbols) are exclusively in the cluster with pleomorphic (Pleo) synaptic vesicles in A and B, but exclusively with the cluster with large, round (Lg Rnd) synaptic vesicles in C. Arrows point to terminals that formed a synapse onto a TTMN or onto MOC neurons but in which the spine was from a small dendrite of unknown source. Not plotted were uncommon terminals (those with vesicles of heterogenous sizes or with a postsynaptic cistern, found only on the motoneurons). Panel A is modified from Benson et al. (2013).

Table 1

Data on Spines.

	TTMN	SMN	MOC neurons
No. spines studied in complete series	9 (10 in partial series)	6	11
No. spines/ soma (calculated[a])	0–40 (*n*=3 somata)	25–30 (*n*=2 somata)	17–19 (*n*=2 somata)
Spine volume (avg., in μm^3)	0.140	0.098	0.065
No. spine- associated terminals	8	4	8
Synapse Position[b]			
Base of spine	4	3	5
Remote from base	3	2	2
Shaft of spine	1	1	0
Tip of spine	1	0	0

[a] See Experimental Procedures for details of calculation.

[b] Synapse closest to spine was used. Spines of unknown origin not used.